Supporting Information

Polarized Ferroelectric Field-Enhanced Self-Powered Perovskite Photodetector

Fengren Cao, Wei Tian, Meng Wang, and Liang Li*

College of Physics, Optoelectronics and Energy, Center for Energy Conversion Materials & Physics (CECMP), Jiangsu Key Laboratory of Thin Films, Soochow University, Suzhou 215006, People's Republic of China

E-mail: lli@suda.edu.cn; liang.li0216@gmail.com

Number of pages: 17

Number of Figures: 13 (Fig. S1-S13)

Number of Tables: 2 (Table S1-S2)

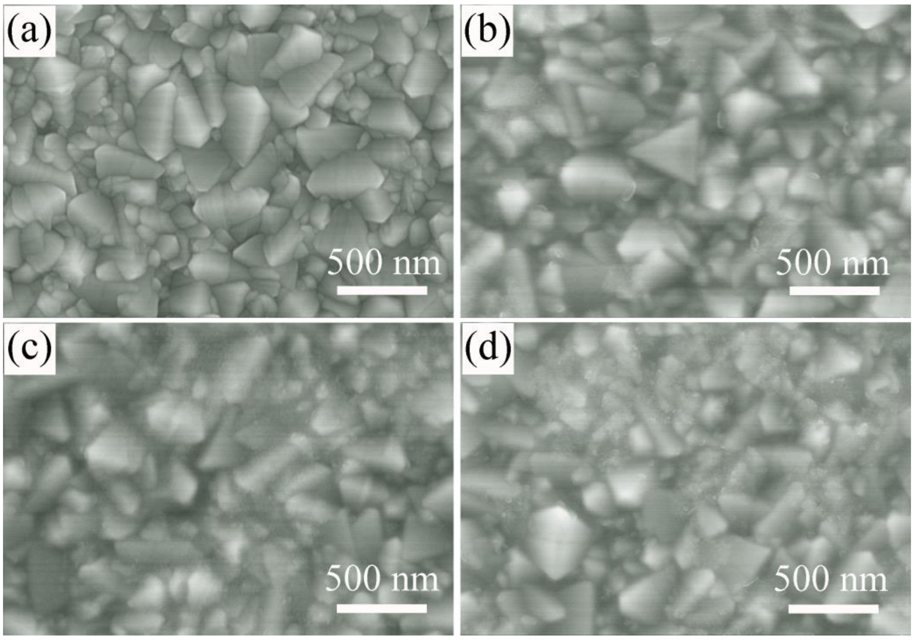

Figure S1. SEM images of (a) FTO, and STO layers with different spin-coated cycles: (b) 1 cycle, (c) 2 cycles, and (d) 3 cycles.

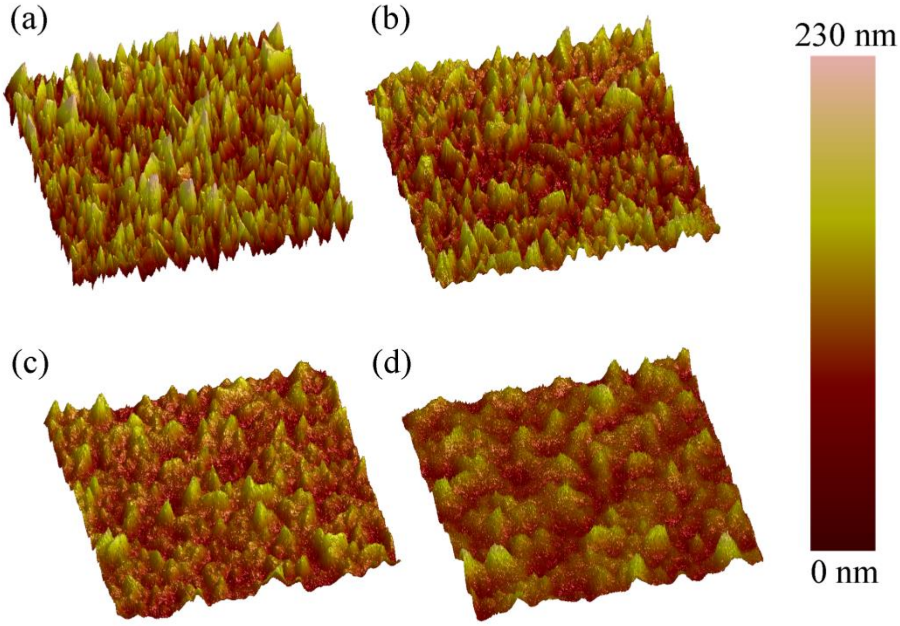

Figure S2. 3D AFM topography images of (a) FTO, and STO layers with different spin-coated cycles: (b) 1 cycle, (c) 2 cycles, and (d) 3 cycles.

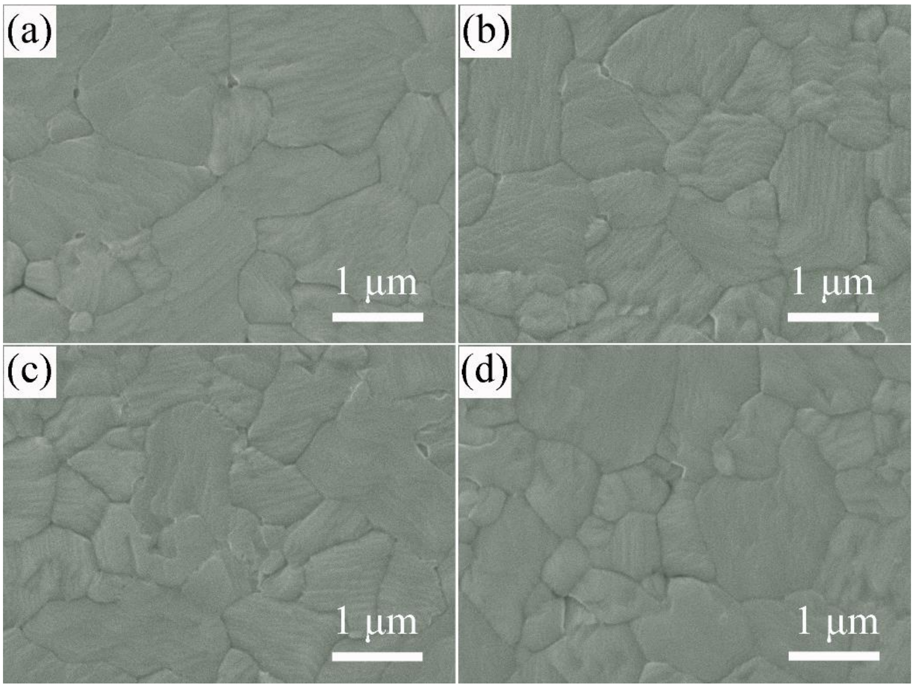

Figure S3. SEM images of (a) perovskite, and STO/perovskite hybrid structure with different spin-coated cycles of STO: (b) 1 cycle, (c) 2 cycles, and (d) 3 cycles.

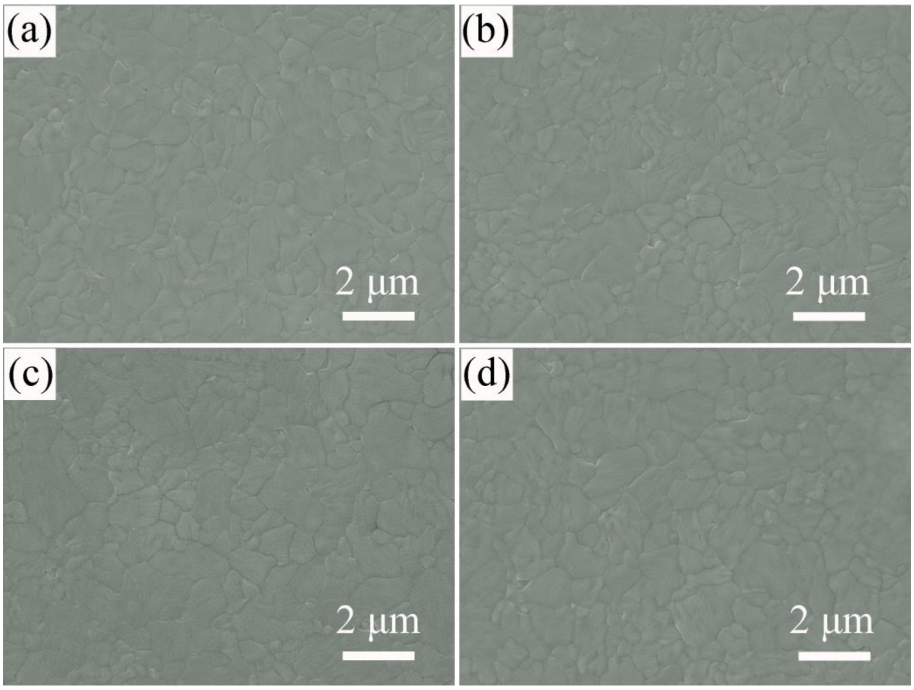

Figure S4. Low-magnified SEM images of (a) perovskite, and STO/perovskite hybrid structure with different spin-coated cycles of STO: (b) 1 cycle, (c) 2 cycles, and (d) 3 cycles.

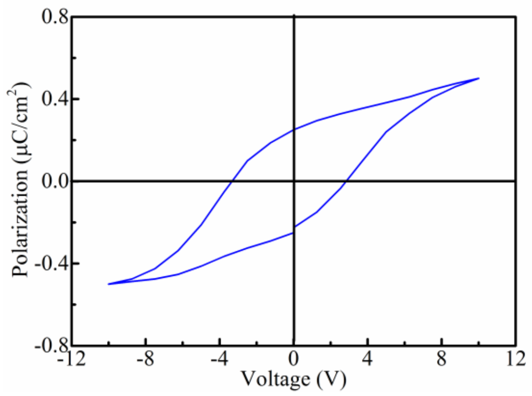

Figure S5. *P*-*V* hysteresis loops of pristine STO film.

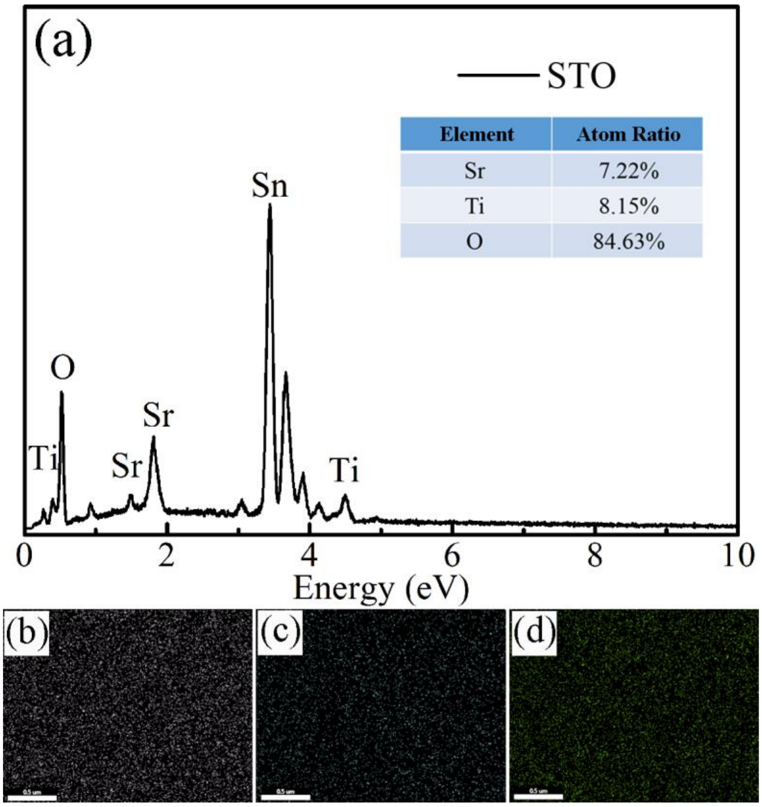

Figure S6. (a) EDX pattern of pristine STO film, and corresponding elemental mapping: (b) Sr, (c) Ti, and (d) O.

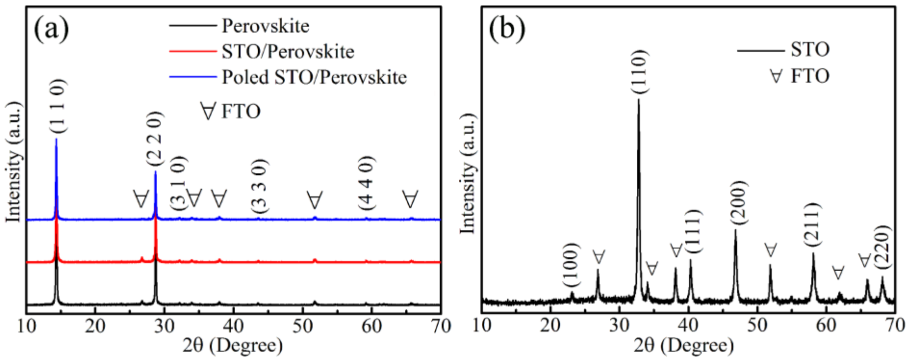

Figure S7. XRD patterns of (a) perovskite, STO/Perovskite, and positively poled STO/Perovskite, and (b) pristine STO film.

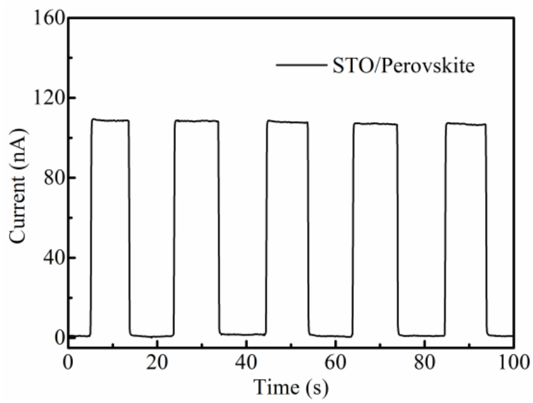

Figure S8. *I-t* curve of the STO/Spiro-OMeTAD photodetector under white light illumination at 0 V.

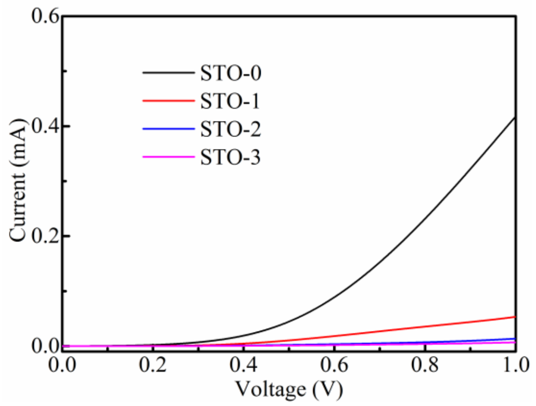

Figure S9. *I-V* curves of all as-prepared STO-x devices in dark.

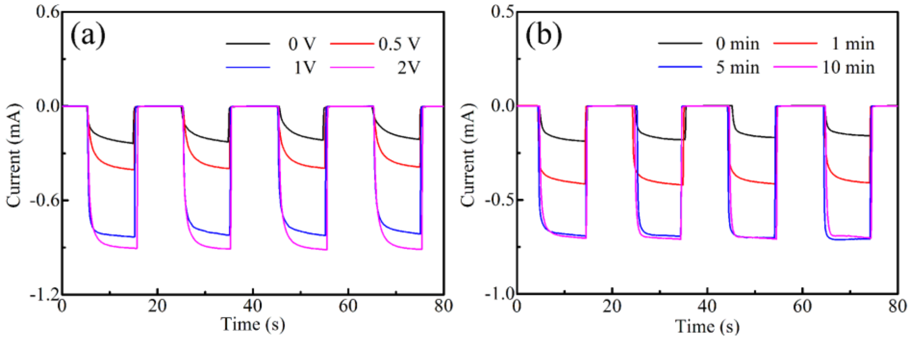

Figure S10. *I*-*t* curves of the as-prepared STO-1 under white light illumination at 0 V with different polarization treatment process: (a) different polarization voltage with certain time of 5 min, (b) different polarization time with certain voltage of 1 V.

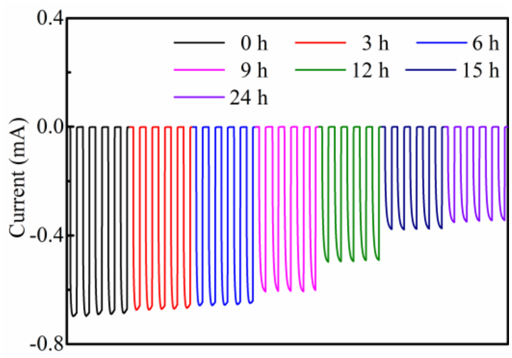

Figure S11. Stability measurement of positively poled STO-1 devices under white light illumination after placing in air for different hours.

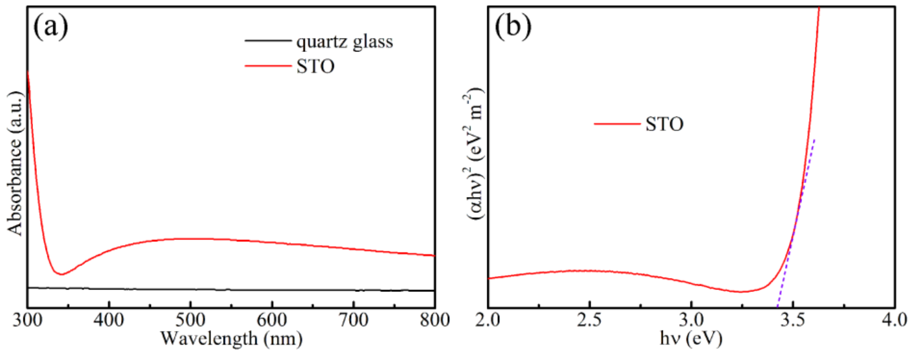

Figure S12. (a) The absorption spectra of pristine STO film and quartz glass. (b) The relationship between the absorption coefficient α and the energy band gap of STO.

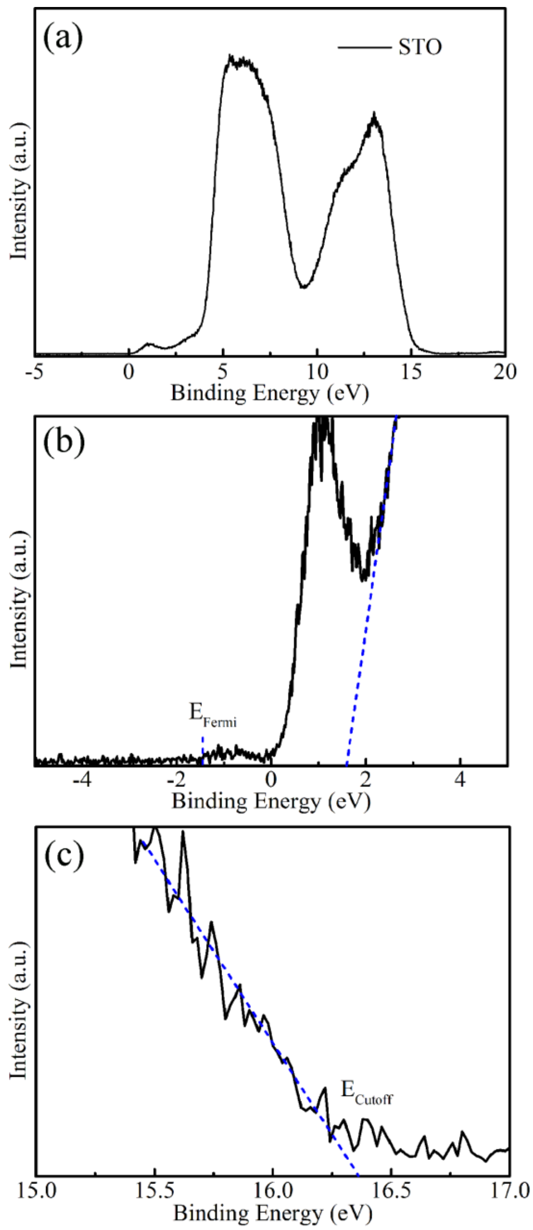

Figure S13. (a) UPS spectrum of STO, and (b-c) locally magnified spectrum of (a).

Table S1. Comparison of the characteristic parameters for perovskite based self-powered photodetectors from previous reports and the present work.

Devices	Light	Rise/Decay time	Responsivity (A/W)	Reference
Au/ $CH_3NH_3PbI_3$/Au	white light (100 mW cm^{-2})	<0.2/<0.2 s	7.92 (4 V)	1
Au/ $CH_3NH_3PbI_3$/Au	(10 μW cm^{-2})	80/80 ms	0.418	2
C_{60}/$CH_3NH_3PbI_3$/GaN	(40 μW cm^{-2})	0.45/0.63 s	0.198	3
PEDOT:PSS/$CH_3NH_3PbI_3$/ PCBM	670 nm	4.0/3.3 μs	0.321	4
$CH_3NH_3PbI_3$/Graphene	560 nm (40 mW cm^{-2})	5 ms	0.375	5
MoO_3/$CH_3NH_3PbI_3$/ZnO	500 nm	0.7/0.6 s	24.3 (500 nm)	6
PTAA/$CH_3NH_3PbI_3$/C_{60}/BCP	White (100 mW cm^{-2})	0.65 ns	0.47 (680 nm)	7
$MAPbBr_3$/$MAPbI_xBr_{3-x}$ heterojunction	450 nm (5 μW)	2.3/2.76 s	11.5 (450 nm)	8
TiO_2/Al_2O_3/PCBM/$CH_3NH_3PbI_3$/Spiro-OMeTAD	600 nm (0.1 mW cm^{-2})	1.2/3.2 μs	0.395 (600 nm)	9
FTO/STO/$CH_3NH_3PbI_3$/Spiro-OMeTAD/Ag	White (100 mW cm^{-2})	0.2/<0.1 s	0.73 (550 nm)	This work

(1) Fang, H.; Li, Q.; Ding, J.; Li, N.; Tian, H.; Zhang, L.; Ren, T.; Dai, J.; Wang, L.; Yan, Q. A self-powered organolead halide perovskite single crystal photodetector driven by a DVD-based triboelectric nanogenerator. *J. Mater. Chem. C* **2016**, *4*, 630-636.

(2) Leung, S. F.; Ho, K. T.; Kung, P. K.; Hsiao, V. K.; Alshareef, H. N.; Wang, Z. L.; He Jr, H. A self-powered and flexible organometallic halide perovskite photodetector with very high detectivity. *Adv. Mater.* **2018,** *30*, 1704611.

(3) Zhou, H.; Mei, J.; Xue, M.; Song, Z.; Wang, H. High-stability, self-powered perovskite

photodetector based on a $CH_3NH_3PbI_3$/GaN heterojunction with C_{60} as an electron transport layer. *J. Phys. Chem. C* **2017**, *121*, 21541-21545.

(4) Bao, C.; Zhu, W.; Yang, J.; Li, F.; Gu, S.; Wang, Y.; Yu, T.; Zhu, J.; Zhou, Y.; Zou, Z. Highly flexible self-powered organolead trihalide perovskite photodetectors with gold nanowire networks as transparent electrodes. *ACS Appl. Mater. Interfaces* **2016**, *8*, 23868-23875.

(5) Li, J.; Yuan, S.; Tang, G.; Li, G.; Liu, D.; Li, J.; Hu, X.; Liu, Y.; Li, J.; Yang, Z.; Liu, S. F. Liu, Z.; Gao, F.; Yan, F. High-performance, self-powered photodetectors based on perovskite and graphene. *ACS Appl. Mater. Interfaces***2017**, *9*, 42779-42787.

(6) Yu, J.; Chen, X.; Wang, Y.; Zhou, H.; Xue, M.; Xu, Y.; Li, Z.; Ye, C.; Zhang, J.; Aken, P. A. V.; Lund, P. D.; Wang, H. A high-performance self-powered broadband photodetector based on a $CH_3NH_3PbI_3$ perovskite/ZnO nanorod array heterostructure. *J. Mater. Chem. C***2016**, *4*, 7302-7308.

(7) Cao, M.; Tian, J.; Cai, Z.; Peng, L.; Yang, L.; Wei, D. Perovskite heterojunction based on $CH_3NH_3PbBr_3$ single crystal for high-sensitive self-powered photodetector. *Appl. Phys. Lett.* **2016**, *109*, 233303.

(8) Shen, L.; Fang, Y.; Wang, D.; Bai, Y.; Deng, Y.; Wang, M.; Lu, Y.; Huang, J. A self-powered, sub-nanosecond-response solution-processed hybrid perovskite photodetector for time-resolved photoluminescence-lifetime detection. *Adv. Mater.* **2016**, *28*, 10794-10800.

(9) Sutherland, B. R.; Johnston, A. K.; Ip, A. H.; Xu, J.; Adinolfi, V.; Kanjanaboos, P.; Sargent, E. H. Sensitive, fast, and stable perovskite photodetectors exploiting interface engineering. *Acs Photonics* **2015**, *2*, 1117-1123.

Table S2. Comparison of the response time and responsivity of STO-0 and STO-1.

Devices	Light	Poling Treatment	Rise/Decay time(s)	Responsivity (A/W)
STO-1	White	No	0.3/<0.1	0.73 (550 nm)
		Positive	0.2/<0.1	
		Negative	2.9/<0.1	
	350 nm	No	6.9/3.0	
		Positive	3.5/2.0	
		Negative	6.1/1.7	
	550 nm	No	2.8/1.5	
		Positive	2.1/1.0	
		Negative	4.9/0.8	
	750 nm	No	4.2/2.4	
		Positive	2.9/1.7	
		Negative	5.3/0.8	
STO-0	White	No	0.2/<0.2	0.31 (550 nm)
		Positive	0.2/<0.2	
		Negative	0.2/<0.2	
	350 nm	No	5.4/2.5	
	550 nm		2.9/0.9	
	750 nm		4.0/1.1	